Crystal Structure of the Metal-bound Superoxide Dismutase from *Pyrobaculum aerophilum* and Comparison with the Metal-free Form

Sangho Lee

Department of Biological Science, Sungkyunkwan University, Suwon 440-746, Korea. E-mail: sangholee@skku.edu
Received October 14, 2008

Superoxide dismutase provides a safeguard against reactive oxygen species by converting toxic superoxide to oxygen and hydrogen peroxide. Biological function of a superoxide dismutase mandates the presence of a metal ion. Previously the crystal structure of the metal-free form of superoxide dismutase from a hyperthermophile *Pyrobaculum aerophilum* (*Pa*SOD) was reported. *Pa*SOD, when expressed as the metal-free form in a bacterial system, is known to incorporate a metal ion by thermal activation. In this study, the crystal structure of *Pa*SOD in its metal-bound form has been determined at 1.85 Å resolution in the space group $P3_221$. The structure exhibits a canonical Mn-or-Fe superoxide dismutase fold with one tetramer in the asymmetric unit. Active site geometry is consistent with those of previously known Mn-or-Fe superoxide dismutase orthologs. Structure comparison of the metal-bound form with the previously determined metal-free form revealed almost identical conformations in overall fold other than the presence of a metal ion in the active site for the metal-bound form. However, subtle changes were observed in the conformations of active site residues and loop residues positioned at the entry to the active site. Such results imply that the structure of *Pa*SOD appears to be rigid against metal incorporation overall with locally confined conformational changes to facilitate the incorporation process.

Key Words : Superoxide dismutase, Metal, *Pyrobaculum aerophilum*

Introduction

Superoxide dismutases (SODs; EC 1.15.1.1) catalyze disproportionation of superoxide to oxygen and hydrogen peroxide.[1] By degrading highly toxic superoxide, SODs provides the cells with a protection mechanism from reactive oxygen species. Biological function of a superoxide dismutase requires the presence of a metal ion. Metal ions such as copper, zinc, manganese, iron and nickel act as crucial cofactors for the proper functioning of SODs. The identity of metal ion(s) serves as the criterion for classifying SOD families: Cu/Zn, Mn-or-Fe and Ni SODs. Mn-or-Fe SODs share structural and sequence similarities among the constituent members.[2] Most Mn-or-Fe SODs mandates a specific ion in their active sites to be active. However, certain number of Mn-or-Fe SODs exhibit activity by either ion in the active site. Such Mn-or-Fe SODs are called cambialistic. To date, only two crystal structures for the cambialistic superoxide dismutase have been reported.[3,4]

SOD from a hyperthermophile *Pyrobaculum aerophilum* (*Pa*SOD) is a cambialistic Mn-or-Fe SODs. *Pa*SOD is active both with manganese and iron but shows higher activity with manganese.[5] Recombinant metal-free *Pa*SOD incorporates metal ion by thermal activation, which is also observed with another thermophilic manganese superoxide dismutase from *Thermus thermophilus*.[6]

In this study the crystal structure of metal-bound *Pa*SOD has been determined at 1.85 Å resolution. Comparison of the metal-bound *Pa*SOD with the previously reported metal-free form reveals that both forms share an almost identical fold except the presence of a manganese ion in the active site of the metal-bound form. However, subtle differences in the conformations of the active site residues in the metal-bound form are observed when compared to those in the metal-free form.

Methods

Expression and purification of the metal-free *Pa*SOD was performed as described previously.[7] The construct contains extra eleven residues at the N-terminus. Residue numbering throughout this report thus accounts for these N-terminal extra residues. Reconstitution of metal-bound *Pa*SOD followed the published procedure[5] with modifications. Briefly, 10-100 mM $MnCl_2$ solution was added to the metal-free *Pa*SOD in 20 mM HEPES pH 7.8, 300 mM NaCl (buffer A) and the resulting solution was incubated at 95 °C for 1 h. The solution was centrifuged at 35,000 *g* to remove any insoluble aggregates and dialyzed in the buffer A supplemented with 2 mM EDTA to remove unbound manganese ions. The resulting solution was dialyzed again in the buffer A and concentrated. Manganese-reconstituted *Pa*SOD in the buffer A was concentrated using a centricon (Amicon) with a molecular weight cutoff of 10,000 Da to 7.1 mg mL^{-1}. The proteins were crystallized by hanging drop vapor diffusion method at 22 °C. Trigonal crystals were grown in reservoir solution containing 0.1 M PIPES pH 7.0, 22% (w/v) polyethylene glycol 3000 and 0.15 M calcium acetate. Crystals appeared within a week. Crystals were flash frozen in liquid nitrogen at −180 °C. The crystal diffracted to resolution limit of 1.85 Å. Data were collected at Brookhaven National Light Source using a Quantum 4 CCD area detector. The datasets were

Table 1. Data Collection and Refinement Statistics

Data Collection	
Space group	$P3_221$
Unit cell parameters	
a (Å)	94.91
b (Å)	94.91
c (Å)	171.89
Number of molecules in the asymmetric unit	4
Beam Source	BNLS[a]
Resolution range (Å)	47.0-1.85
Total reflections	828,724
Unique reflections	76,717
Completeness (%)	99.4 (99.6)
R_{merge} (%)[b]	7.6 (51.8)
$<I/\sigma>$[c]	23.2 (3.7)
Refinement	
Resolution range for refinement (Å)	47.0-1.85
Number of protein atoms	7,038
Number of other molecules	
Manganese	4
Water	178
Average B-factor, (Å^2)	
Protein atoms	30.6
Manganese	41.1
R.m.s.d.	
Bond length (Å)	0.009
Bond angle (°)	1.08
R_{free}[d]/R_{work}	0.230/0.202

Numbers in parentheses are the numbers in the highest resolution shells. [a]BNLS: Brookhaven National Light Source beamline X8C. [b]$R_{merge} = \Sigma_{hkl}\Sigma_i \mid I(hkl)_i - <I(hkl)> \mid / \Sigma_{hkl}\Sigma_i <I(hkl)_i>$. [c]$<I/\sigma>$ values are calculated from the outputs in the program *SCALEPACK*.[8] [d]R_{free} is calculated for a randomly chosen 10% of reflections.

processed using *DENZO* and *SCALEPACK*.[8] Data collection and processing statistics are shown in Table 1. The molecular-replacement solution was found assuming the point group $P321$ with the program *AMoRe*[9] using a tetramer from the metal-free form of *Pa*SOD as a search model (PDB ID: 1P7G). The Matthew's coefficient (V_m)[10] was suggested to be 2.31 Å^3/Da, assuming one tetramer in the asymmetric unit. The cross-rotation function calculations yielded the top peak with the correlation coefficient of 11.7% and the R-factor of 61.9%. The translation function calculations suggested $P3_221$ as the correct enantiomorph for the top peak with the correlation coefficient of 37.6% and the R-factor of 49.4%. Rigid-body refinement of the top solution yielded the correlation coefficient of 44.0% and the R-factor of 48.6%. No non-crystallographic symmetry restraint or constraint was used in the final stages of refinement. Interactive model building was performed in *O*[11] and *Coot*[12] and initial models were refined with *CNS*.[13] In an early stage of structure determination anomalous Fourier map was calculated on a dataset different from the dataset for final refinement using *CCP4* suite[14] to locate manganese sites. Final stages of the refinement were performed using *Refmac5* with TLS implemented.[15] Refinement statistics are shown in Table 1. Structure factors and atomic coordinates have been deposited in Protein Data Bank with an access code 3EVK.

Results and Discussion

The structure of the metal-bound *Pa*SOD consists of two subdomains (Fig. 1A and B). The N-terminal subdomain harbors two long helices and one long and one short loop. At the N-terminus, a long loop (L1) runs parallel to a long helix H1. The L1 is followed by the helix H1. The second helix (H2) is connected to H1 with a short loop (L2). Conserved Pro23 is a *cis*-peptide. The C-terminal subdomain shows an α/β fold with 4 helices (H3, H4, H5 and H6) and 3 strands (S1, S2 and S3). In the metal-bound *Pa*SOD structure, the manganese is located between the two subdomains. The overall fold of the metal-bound *Pa*SOD is similar to that of other known Mn-or-Fe SODs, which is expected from sequence similarity (Fig. 1C). For instance, *Pa*SOD exhibits 55% sequence identity with Fe SOD from *Sulfolobus solfactaricus*[16] (PDB: 1SSS). Another group presented the determination of the *Pa*SOD complexed with manganese in a scientific meeting.[17] However, no *Pa*SOD structure from this group has ever been deposited to the protein data bank, nor has any regular scientific paper describing the metal-bound *Pa*SOD structure been published.

The metal-bound *Pa*SOD crystals show tetrameric arrangements as in the case of the metal-free *Pa*SOD.[7] The metal-bound *Pa*SOD tetramer exhibits canonical 222 symmetry (Fig. 1D). The asymmetric unit contains four monomers, forming a tetramer. In contrast, the asymmetric unit of the metal-free form crystal harbors six tetramers, resulting in 24 monomers.[7] In the crystal of the metal-bound form, two distinct sets of monomers were observed: the first set, comprising chains A and C, is better ordered than the second set, comprising chains B and D (Fig. 1B).

There are subtle differences between the metal-bound and the metal-free forms of *Pa*SOD although the overall folds of the two forms are almost identical (Fig. 2A). The overall r.m.s. distance of the tetramer is 0.30 Å when all the atoms in the tetramer of the metal-bound structure are superimposed to the corresponding tetramer of the metal-free structure. Small but noticeable backbone differences are detected in L2 as well as both N- and C-termini (Fig. 2A). To characterize subtle changes in the backbone between the metal-bound and the metal-free *Pa*SOD structures in details, difference distance matrices (DDMs) are calculated.[18] DDMs were calculated for all four chains in the asymmetric unit of the metal-bound structure in reference to the A chain of the metal-free form (PDB ID: 1P7G) using *DDMP* (Yale University). In the chains B and D of the metal-bound structure, residues 100 to 103 show the largest difference distances (Fig. 2A). Residues 100 to 103 are mapped in the loop between H2 and H3. This region connects the two subdomains and is located at the front of "gate" to the active site. The maximum difference distance for the backbone in the residues 100 to 103 is 3.3 Å. Such difference distance

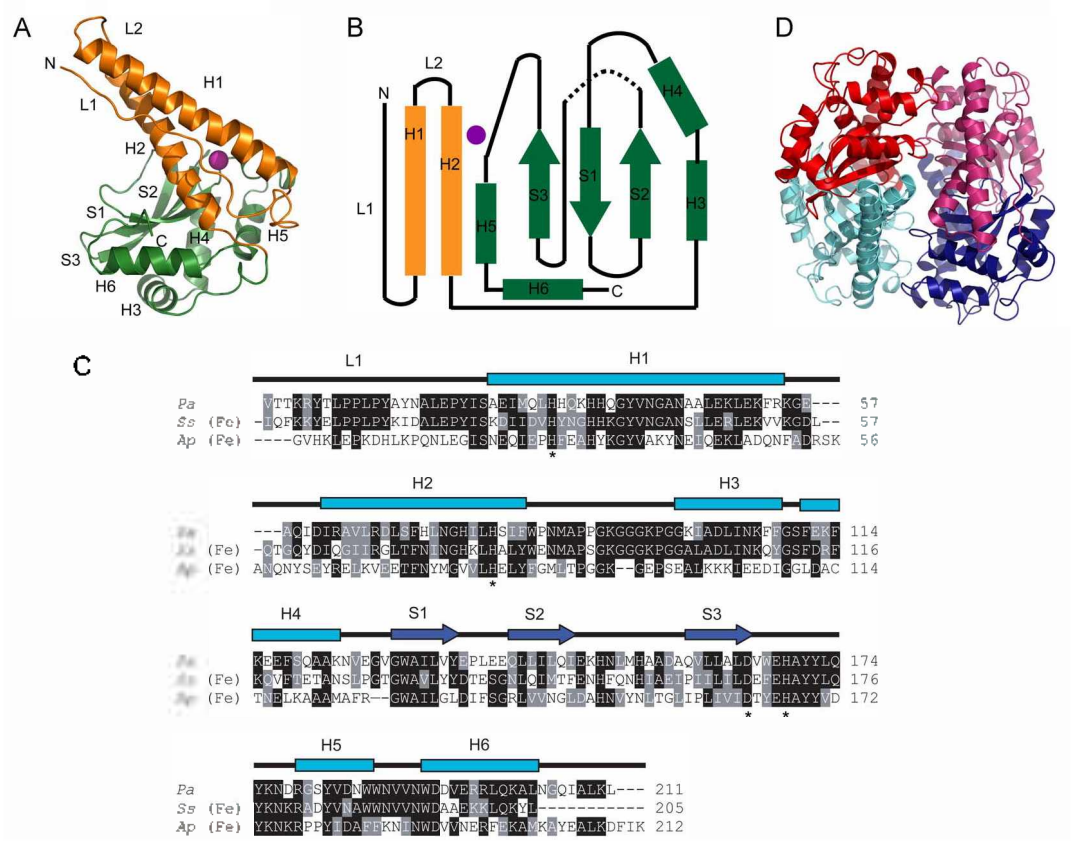

Figure 1. (A) Structure of the metal-bound *Pa*SOD monomer. The N- and C-termini are labeled. N-terminal and C-terminal subdomains are depicted as orange and green, respectively. The manganese is shown as a purple sphere. Secondary structural elements are labeled; H, helix; S, strand; L, loop. (B) Topology of the metal-bound *Pa*SOD monomer. The same coloring scheme as (A) is used to designate the subdomains. (C) Structure-based multiple sequence alignment of Mn-or-Fe SODs. *Pa*, *Pyrobaculum aerophilum*; *Ss*, *Sulfolobus solfataricus*; *Ap*, *Aquifex pyrophilus*. Secondary structures of *Pa*SOD are indicated above the alignment with active site residues depicted as asterisks (*). (D) The metal-bound *Pa*SOD tetramer. Chains A and C are colored in blue and cyan, respectively. Chains B and D are presented in red and pink, respectively. Manganese atoms are shown as spheres with the same color as the chain each manganese atom belongs to. This figure was prepared by PyMol (http://www.pymol.org).

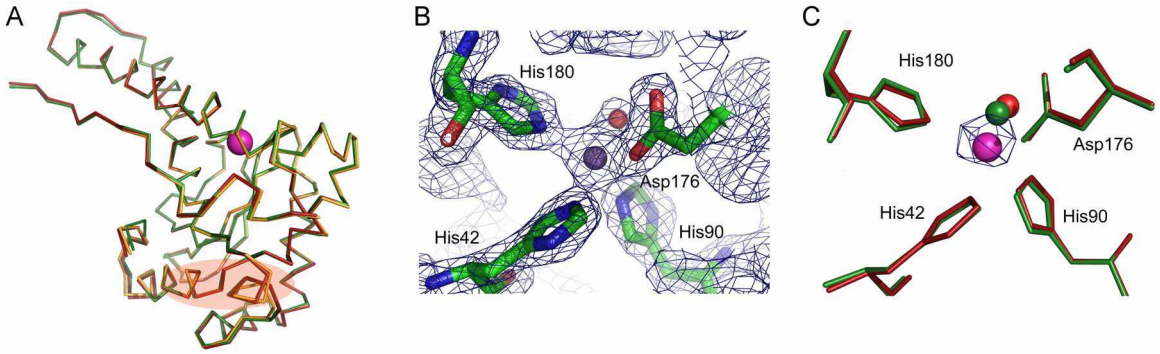

Figure 2. (A) Comparison of the overall fold in the metal-free and the metal-bound *Pa*SODs. Cα traces for the metal-free (green), chains A (red) and B (orange) of the metal-bound forms are shown. Manganese atom is depicted as a magenta sphere. The direction of the figure is the same as Fig. 1A. The region suggested to be the relatively significant backbone movement is indicated as a pale red oval. (B) 2*Fo*-*Fc* map for the active site of the metal-bound *Pa*SOD is shown at 2σ contour level along with the active site residues in stick model. The conserved solvent molecule in the active site is described in red. Manganese atom is represented as a magenta sphere. (C) Comparison of the active site between two forms of *Pa*SOD. Active site residues and the conserved solvent molecule from the chain A of the metal-free form (green) and from the chain A of the metal-bound form (red) are presented in stick model. Peak for the manganese (magenta sphere) calculated from anomalous Fourier difference map (see Methods for details) is shown at 4σ contour level at 2.7 Å resolution. This figure was prepared by PyMol (http://www.pymol.org).

implicates that local subtle conformational change may play a limited role in metal incorporation.

The active site of the metal-bound *Pa*SOD reveals a bipyramidal coordination of the manganese ion with four

Table 2. Distances from the center molecule to key residue atoms in the active site of *Pa*SOD

Structure	Metal-free	Metal-bound					Mn(Avg)[a]
Center atom	OH_2[b]	Mn					Mn
Chain		A	B	C	D	Average[c]	
His42 Nε2	3.78 ± 0.14	2.26	2.11	2.12	2.31	2.20 ± 0.10	2.12 ± 0.03
His90 Nε2	3.25 ± 0.22	2.32	2.47	2.38	2.09	2.32 ± 0.16	2.13 ± 0.03
Asp176 Oδ2	2.60 ± 0.26	2.02	1.75	2.06	2.50	2.08 ± 0.31	1.92 ± 0.10
His180 Nε2	2.77 ± 0.09	2.39	2.48	2.40	2.32	2.40 ± 0.07	2.21 ± 0.04
OH[d]	N/A	1.95	2.24	1.90	N/A	2.03 ± 0.18	2.14 ± 0.16

All distances are in Å. The averaged distances from all the subunits in the asymmetric unit (4 subunits in the metal-bound forms and 24 subunits in the metal-free form) are listed. [a]Average refers to the averaged distances calculated from eight different Mn-or-Fe SODs.[16] [b]OH_2 refers to the solvent molecule that occupies the metal position in the active site of the inactive form. [c]OH refers to the coordinating solvent molecule that has been suggested to be a hydroxide ion. [d]The average distance and the standard deviation were calculated from three out of four subunits in the asymmetric unit.

amino acid side chains and a water or hydroxide ion, which is a recurring theme in the Mn-or-Fe SOD family (Fig. 2B). Differences other than the presence of a metal ion are observed in the active sites of the metal-bound and the metal-free *Pa*SOD structures (Fig. 2C). In the metal-bound *Pa*SOD, a manganese ion is coordinated by four conserved residues (His42, His90, Asp176 and His180) and a conserved solvent molecule. The conserved solvent molecule has been suggested to be either water or a hydroxide ion.[19] In the metal-free *Pa*SOD, only the solvent molecule is observed in the active site.[7]

Distances from a manganese ion to coordinating atoms are consistent with those found in other SOD active sites (Table 2). In the metal-free *Pa*SOD, however, the distances from the water molecule to potential coordinating atoms are longer than those in the metal-bound *Pa*SOD. His42 and His 90 show the largest differences in the distances from the metal or the water molecule between the metal-bound and the metal-free *Pa*SODs. In His42, the distance from Nε2 to the manganese ion in the metal-bound *Pa*SOD is 3.78 Å while the distance from Nε2 to the water molecule in the metal-free form is 2.20 Å. In His90, the distances from Nε2 to the manganese ion and the water molecule are 2.32 Å and 3.25 Å, respectively. Residues around the active site belong to first or second hydration shells.[20] Whittaker and Whittaker predicted that in *Pa*SOD, a histidine residue would occupy a position as an outer-sphere hydrogen bonding donor, which is occupied by glutamines in many Mn or Fe-specific SODs.[5] Indeed His 161 Nε2 forms a hydrogen bonding with the conserved water molecule bound to the manganese ion (distance: 3.2 Å).

In summary, the crystal structure of the metal-bound *Pa*SOD reveals almost identical structure with that of the metal-free form. Despite of the overall similarity of fold between two forms of *Pa*SOD, subtle differences are noted. Comparison of the metal-bound *Pa*SOD from the metal-free form suggests that *Pa*SOD structure is rigid such that the incorporation of the metal into the active site results in almost identical conformation. The results from the present study imply that simple static structural studies are insufficient to elucidate a possible mechanism for incorporating a metal into the active site of *Pa*SOD although local conformational changes may facilitate the metal incorporation. Obviously elegant experiments beyond simple crystallographic studies would resolve metal incorporation mechanisms previously hypothesized[19] for *Pa*SOD and SODs in general.

Acknowledgments. The author thanks Dr. David Eisenberg and Dr. Michael R. Sawaya for their valuable guidance in the early stages of this work. This work was supported by the Faculty Research Fund, Sungkyunkwan University, 2007 to S. L.

References

1. Fridovich, I. *Annu. Rev. Biochem.* **1995**, *64*, 97-112.
2. Wintjens, R.; Noel, C.; May, A. C.; Gerbod, D.; Dufernez, F.; Capron, M.; Viscogliosi, E.; Rooman, M. *J. Biol. Chem.* **2004**, *279*, 9248-9254.
3. Schmidt, M.; Meier, B.; Parak, F. *J. Biol. Inorg. Chem.* **1996**, *1*, 532-541.
4. Surgio, S.; Hiraoka, B. Y.; Yamakura, F. *Eur. J. Biochem.* **2000**, *267*, 3487-3495.
5. Whittaker, M. M.; Whittaker, J. W. *J. Biol. Inorg. Chem.* **2000**, *5*, 402-408.
6. Whittaker, M. M.; Whittaker, J. W. *J. Biol. Chem.* **1999**, *274*, 34751-34757.
7. Lee, S.; Sawaya, M. R.; Eisenberg, D. *Acta Cryst.* **2003**, *D59*, 2191-2199.
8. Otwinowski, Z.; Minor, W. *Methods Enzymol.* **1997**, *276*, 307-326.
9. Navaza, J. *Acta Cryst.* **1994**, *A50*, 157-163.
10. Matthes, B. W. *J. Mol. Biol.* **1968**, *33*, 491-497.
11. Jones, T. A. *J. Appl. Cryst.* **1978**, *11*, 268-272.
12. Emsley, P.; Cowtan, K. *Acta Cryst.* **2004**, *D60*, 2126-2132.
13. Brunger, A. T.; Adams, P. D.; Clore, G. M.; Gros, P.; Grosse-Kunstleve, R. W.; Jiang, J.-S.; Kuszewski, J.; Nilges, N.; Pannu, N. S.; Read, R. J.; Rice, L. M.; Simonson, T.; Warren, G. L. *Acta Cryst.* **1998**, *D54*, 905-921.
14. Project, C. C. *Acta Cryst.* **1994**, *D50*, 760-763.
15. Winn, M.; Isupov, M.; Murshudov, G. N. *Acta Cryst.* **2001**, *D57*, 122-133.
16. Ursby, T.; Adinolfi, B. S.; Al-Karadaghi, S.; De Vendittis, E.; Bocchini, V. *J. Mol. Biol.* **1999**, *286*(1), 189-205.
17. Jameson, G. B.; Adams, J. J.; Hempstead, P. D.; Anderson, B. F.; Morgenstern-Badarau, I.; Whittaker, J. W.; Baker, E. N. *J. Inorg. Biochem.* **2003**, *96*, 70 (Abstr.).
18. Richards, F. M.; Kundrot, C. E. *Proteins* **1988**, *3*, 71-84.
19. Whittaker, J. W. *Biochem. Soc. Trans.* **2003**, *31*(6), 1318-1321.
20. Edwards, R. A.; Whittaker, M. M.; Whittaker, J. W.; Baker, E. N.; Jamesson, G. B. *Biochemistry* **2001**, *40*, 15-27.